Master's Thesis

Vision-based vibration measurement using speckle pattern and system identification using autoregressive model

Kyeong-Taek Park

Department of Urban and Environmental Engineering
(Disaster Management Engineering)

Graduate School of UNIST

2017

Vision-based vibration measurement using speckle pattern and system identification using autoregressive model

Kyeong-Taek Park

Department of Urban and Environmental Engineering
(Disaster Management Engineering)

Graduate School of UNIST

Vision-based vibration measurement using speckle pattern and system identification using autoregressive model

A thesis/dissertation
submitted to the Graduate School of UNIST
in partial fulfillment of the
requirements for the degree of
Master of Science

Kyeong-Taek Park

1. 16. 2017

Approved by

Advisor
Marco Torbol

Vision-based vibration measurement using speckle pattern and system identification using autoregressive model

Kyeong-Taek Park

This certifies that the thesis/dissertation of Kyeong-Taek Park is approved.

1/16/2016

Advisor: Marco Torbol

Sung-Han Sim: Thesis Committee Member #1

Young-Joo Lee: Thesis Committee Member #2

Abstract

Non-contact sensing techniques are a currently active and vibrant research field on structural health monitoring community because they are cost efficient and simple to use in test field. The non-contact sensors reduce expenses and installation process because they enhance the accessibility of a harsh structural spot that are difficult to approach. Many researchers have studied non-contact sensing techniques to solve civil engineering problems, such as: a non-contact laser ultrasonic scanning system visualizing the cracks at a distance, and a vision-based measurement to measure the displacement signal at a remote place.

This study introduces a new non-contact sensing technique for vision-based displacement measurement. Some researchers have already focused on vision based displacement measurement. They utilized target panels or robust objects as the reference point and their device successfully detected the movement of either target panels or robust objects. The displacement signal obtained by their vision-based measurement gave satisfactory resolution to the dynamic properties of the target structure. The new method proposed in this study doesn't require a physical reference point but it utilizes laser speckle pattern to create the optical reference point.

The speckle pattern occurs when a coherent red light is diffusely reflected on a rough surface. The set of scattered photons from the specular surface is called the speckle pattern. In this study, the laser beam is spread over a target structure surface. Under the constant incident ray, a slight tilt of the target surface changes an incidence angle. The diffusely reflected rays, speckle patterns, intensively react against the small movement of the target. A camera outside of the target structure records the sensitive response due to the vibrations in real time. The movement of the target due to ambient vibrations is estimated by image processing algorithms, such as: the laser speckle contrast imaging for detecting the movement, and *k*-means clustering for estimating virtual nodal points.

The two consecutive algorithms estimate the actual displacement. The laser speckle contrast analysis (LASCA), which is popular methods to visualize blood flow in biomedical community, quantifies the blurring extent of each raw speckle image. Because the blurring represents the motion during a camera exposure, the movements of the target in stationary images is digitalized by LASCA. With speckle contrast images in chronological sequence, tracking a single pixel in different images is infeasible. This study utilizes the *k*-means clustering algorithm. The displacement signal is estimated by linking the location of *k* clusters centroids in each interval. The computed displacement signal in time domain is decomposed to frequency domain by frequency domain transformation techniques such as: frequency domain decomposition, or stochastic subspace identification. This study utilizes both eigendecomposition for system identification and frequency domain decomposition.

To validate the method two lab scale experiments were done; one was done with a shaker and a steel

plate and the other was done with a small steel beam model. In the first experiment, the steel plate on the shaker was vibrating under assigned frequency. The laser beam was spread over the steel plate and the camera recorded the speckle pattern created. The purpose of the experiment was to prove that the speckle pattern recognition algorithms exactly reflect the dynamic property of the vibrating target. In the second experiment with a small steel beam model, the laser was shot on the center of the beam. The purpose of this experiment was to check if the speckle pattern could detect and reflect ambient vibration. These two experiments prove that the speckle pattern recognition method can identify the vibrations of the targets.

Contents

Figures

Tables

I. Introduction

1.1 Background and motivation

As civilization advances, people are building more elaborate and large-scale infrastructures such as: long span bridges spanning a strait, massive airports for international exchange, and skyscrapers which enable urban concentrated business activity. There is no doubt that the progress of construction technology directly or indirectly contributes to modern economic development. However, civil infrastructures inevitably encounter external risks in the form of a load condition and the building collapse leads to huge disasters. Not only does it cost rebuilding expense, but the long-term economic losses due to the absence of the main civil infrastructure are also tremendous. In order to avoid such losses, it is necessary to inspect structures in advance and to diagnose their status. The process of assessing structural status and detecting the damage inside is called structural health monitoring (SHM) (Sohn et al., 2003).

To secure the structural safety for public availability, the SHM techniques have been intensively developed over the last couple decades. At the center of these developments were technical improvements of wireless sensor networks (Lynch & Loh, 2006). Wireless sensors have the merits of convenient and relatively inexpensive installation compared to traditional tethered monitoring systems and autonomous data processing performance by an embedded computing unit. With the data acquired by sensors attached on a structure, civil engineers process it and exploit it for detecting damage extension within a structure as well as diagnosing a structural condition. The more sensing technology advances, the better the SHM techniques are efficiently applied to civil engineering problems. Consequently, the SHM and wireless sensor technology have promoted securing structures against the forthcoming danger within civil structures.

As mentioned above, wireless sensing technology has advantages of its simple and convenient deployment in test field and autonomous data processing capability. Since the wireless sensing technology was invented, it has become easy to install a large number of wireless sensors on structures and they effectively collect the data in accordance with their own purposes respectively. Generally, the purpose of the SHM with wireless sensing is divided into two types based on the scope of target system; one is a local scale SHM and the other is a global scale SHM (Chang, Flatau, & Liu, 2003). While the local scale inspection focuses on partial defects such as crack propagations detection with ultrasonic guided wave, the global scale sensing network takes into account dynamic behavior of a full scale structure. Based on different purposes, sensors are widely utilized in the field of the SHM to obtain useful information from civil structures.

Though the wireless sensing network has overcome past weaknesses of tethered sensing system, it still has several limitations due to its physical characteristics as a contacting sensing unit. In order to

inspect the response of the whole structure, a large number of sensors spread over the structure are required to be arranged systematically to collect vibration data of each nodal point. If someone inspects a long span bridge structure like Yi Sun-sin Bridge, which has its main span length of 1,545 m, not only are hundreds of sensing unit required for full scale inspection but hundreds of people should be allocated for collaborating on the test field. A need for a great number of sensors and manpower leads to great expense for a single inspection of huge structures. Besides cost, physical attachment has limitation when it is required to measure the data on tough conditions. It would be considerably troublesome if the vibration data of the cable suspended between towers of Yi Sun-sin Bridge were required to be obtained and the spot to attach wireless sensing unit were not favorable due to humidity or any other undesirable conditions.

Recently, the SHM technology is not just relying on physical sensors but the SHM techniques also involve non-contacting sensors for its applications. As an alternative to physical sensors, the SHM techniques with non-contacting sensing method have currently been invented for various SHM applications such as: non-contact ultrasonic inspection and vision-based displacement measurement. For example, non-destructive evaluation technique for crack visualization using noncontact laser ultrasonic scanning system has been developed (An, Park, & Sohn, 2013) and vision-based displacement measurement has been performed using target panel and video camera (Lee & Shinozuka, 2006). The advantage of noncontact sensing techniques mostly comes from the convenient and cost efficient measuring system of them.

1.2 Purpose of the study

This study suggests the vision-based vibration response acquisition methodology with neither physical sensing mediums nor target panels. Taking into account merits of non-contact vision-based observation, the proposed methodology doesn't require any kind of physical references for movement recognition. This study utilizes laser speckle pattern recognition analysis instead of placing a target panel on a target structure. Laser speckle contrast analysis (LASCA) (Briers & Webster, 1996), which has been studied by biomedical engineering community, is applied to the SHM application. Laser beam is shot on the target and diffusion level brand camera records vibration response of the speckle patterns created by diffused reflection between laser beam and the target surface. As a result, the SHM application using speckle pattern analysis promises benefits of both cost efficiency and simple applicability.

The procedure of the whole study is divided into three parts. Figure 1 shown in the following page describes overall flow chart of the study. First, the laser speckle patterns captured in real time are converted to speckle contrast image one by one. Second, the *k*-means clustering algorithm (Hartigan & Wong, 1979) tracks the movement of targets by calculating clusters' centroids for each photo frame. Finally, modal analysis techniques such as frequency domain decomposition (FDD) (Brincker, Zhang, & Andersen, 2000) and system identification using autoregressive (AR) model (Park, Kim, & Torbol, 2016) derive modal parameters as a result. Two lab scale experiments are reported to validate the theoretical descriptions. One is done with a shaking instrument of controllable exciting frequency in order to validate the laser speckle based SHM application proposed. The speckle pattern analysis will be verified if the displacement signal obtained by the methodology precisely reflects exciting frequency. The other experiment is targeting a small steel bridge model and modal analysis results of both FDD and system identification using AR model are compared to validate each other. This experiment addresses that the speckle pattern recognition algorithm successfully detects ambient vibration.

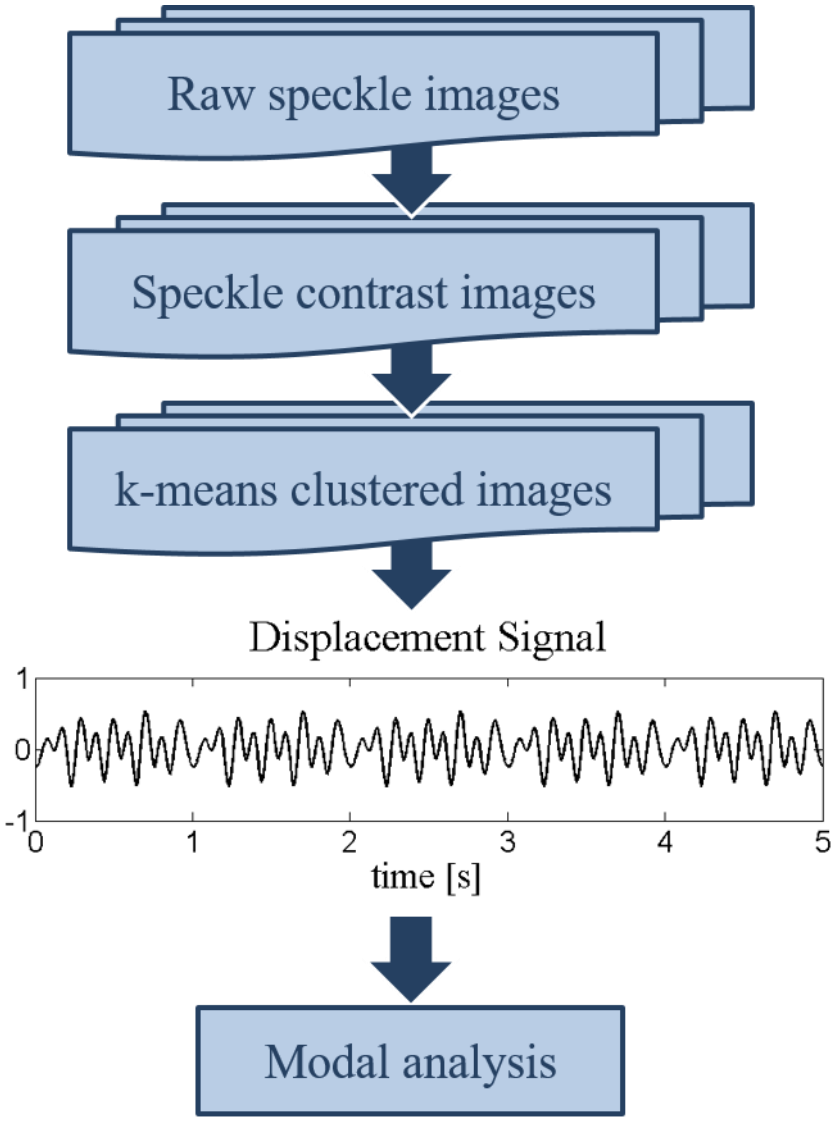

Figure 1 Overall flow chart of the speckle pattern recognition process

II. Speckle pattern analysis

Speckle pattern is generated when a coherent light is randomly interfered by the diffused reflection with scattered medium. It has been widely applied in different engineering fields such as: laser holographic interferometry (Vest, 1979), dynamic speckle processing (Rabal & Braga Jr, 2008) and bending moment (Leendertz & Butters, 1973), deflections (Köpf, 1972) or strain measurement (Yang & Ettemeyer, 2003). Speckle pattern analysis in this study is motivated by blood flow monitoring technique in biomedical engineering field (Dunn, Bolay, Moskowitz, & Boas, 2001). Since laser speckle contrast imaging technique was introduced to biomedical community in 1980s it has become one of the most effective methods to visualize blow flow images. By utilizing speckle contrast imaging technique, it is possible to perceive tiny spatial changes.

This study exploits speckle pattern as a sensing technique. Figure 2 illustrates the speckle pattern recognition applied in this study. Once the laser beam, which is coherently emitted light, spread over the area of the target system, speckle pattern is scattered around a specular surface due to a diffused reflection. The speckle pattern sensitively reflects the small spatial movement so it minutely represents an ambient vibration of the target. While laser light is shot on the target object, the speckle patterns created are recorded by a camera in real time. The raw speckle images obtained are transferred to CPU for following vibration detecting algorithms.

There are two significant processes after obtaining raw speckle pattern images; the first is speckle contrast imaging and the other is the *k*-means clustering algorithm. By applying speckle contrast imaging, the blurring extent of a raw speckle image is quantified (Goodman, 1976) and the movement of the stationary image frame is digitized. Since the speckle contrast image effectively reflects the blurring effect in an image, it enables to represent the changes of the target taken by a camera better than the raw speckle image does. The next step is to track the movement of the target with time. Since the speckle image as a sensing device does not include physical nodal point and it is almost impossible to track the movement of single pixel in different image frames, it is supposed to estimate virtual nodal points which movement would be regarded as displacement of a target. In this study, the *k*-means clustering algorithm is adopted to realize the virtual nodal points in speckle images. The centroids of clusters play role as a nodal points. Tracing the clusters' centroids in every frame with time, their movements are considered to be displacements of the target. Finally, the speckle pattern recognition algorithm composed of speckle contrast imaging and the *k*-means clustering algorithm successfully estimate the displacement of a target object with time.

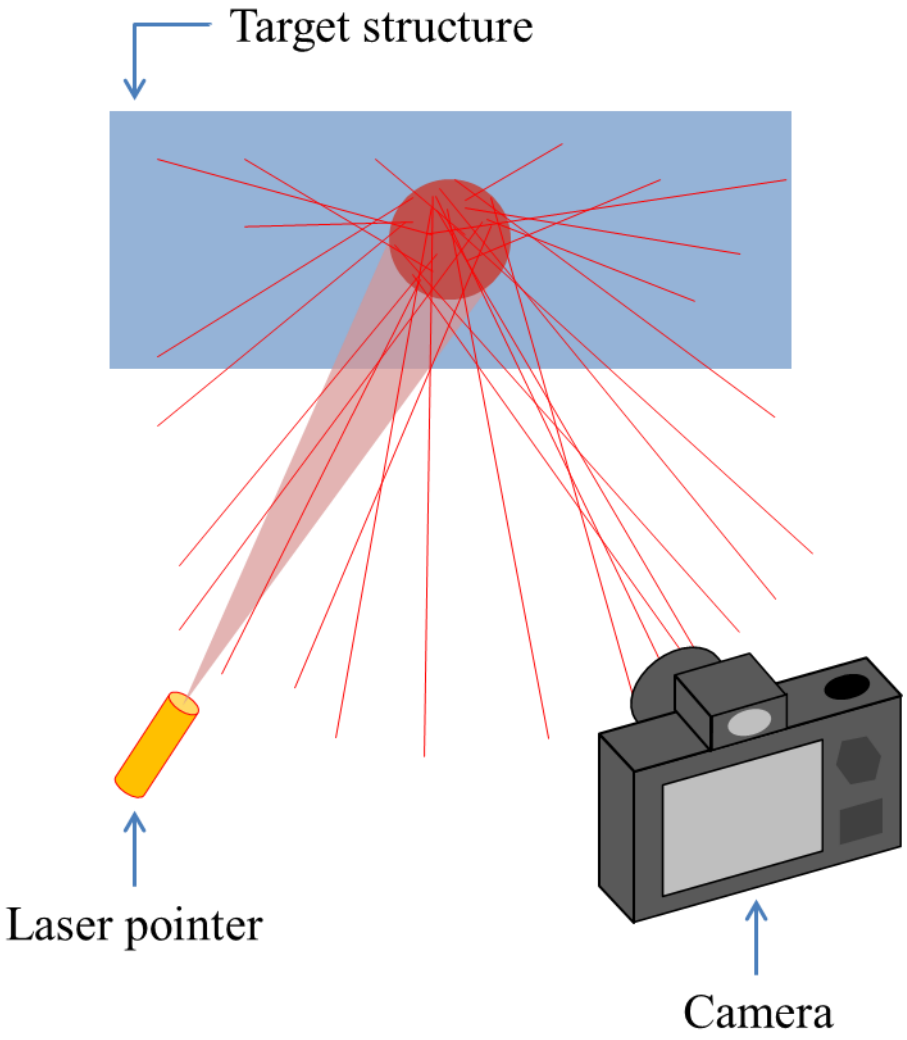

Figure 2 Laser speckle pattern acquisition system and diffused reflection on a specular surface

2.1 Speckle contrast imaging

A single raw speckle pattern image taken with certain frame rate is a snapshot which depicts the vibration of the target object at that instant. The red filter may be used to transmit red light only while eliminating the other lights. The red filtered light efficiently involves the diffusely reflected red light emitted on the specular surface. The photographic exposure time causes the blurring effects on a photo if the target illuminated by the laser beam is vibrating. Even ambient vibration of the target affects the speckle pattern in the form of blurred extent because the reflected laser light sensitively response to extremely tiny changes of the angle of reflection. The blurring effect on a photo states that the target object is moving at the moment of the photographic exposure.

Since the movement of a target object is denoted by the blurring effect, if the blurring effect is digitized, it is possible to highlight the moving object on photo frames. This study utilizes speckle contrast imaging to quantify the blurring phenomenon. The speckle contrast imaging for representing the degree of blurring effect in a specific pixel is defined as:

$$C \equiv \frac{\sigma_I}{\langle I \rangle} \tag{1}$$

Where σ_I is the standard deviation of speckle intensities of surrounding pixels and $<I>$ is the mean of speckle intensities of surrounding pixels.

The speckle contrast value of a specific pixel is computed by the standard deviation divided by the mean of the surrounding pixel window as shown in equation (1). In the stationary speckle patterns, the speckle intensity $p(I)$ appears to be a negative exponential distribution. The speckle contrast value, therefore, is going to be one because the standard deviation in this case is equivalent to the mean value. If the target object is moving, the blurring effect will be taken place in the photo recorded with an exposure and the standard deviation of speckle intensity surrounding a pixel will decline. By quantifying the movements in the photographic images, the speckle contrast imaging enables to distinguish the moving object from static backgrounds. As a result of target's vibration, the blurring occurs in the photo and it brings up the speckle contrast value lower.

2.2 *k*-means clustering algorithm

The speckle contrast imaging successfully determine if an image includes movements in the form of blurring effect. However, the speckle contrast images themselves don't state the displacement because they don't retain any nodal points, which could be criteria to measure the movement with time. Since it is not feasible to achieve one-to-one correspondence between pixels in different images, the optimization algorithm for assigning virtual nodal point is needed to be included in the study. The *k*-means clustering algorithm, which is a popular classification algorithm, is one of solutions. Though there exist various algorithms, which would perform similar functional achievement for classification, the *k*-means clustering algorithm is chosen due to its plain and clear execution. In this study, the centroids of each cluster are regarded as a virtual nodal point, which movement is considered to be the displacement of the node.

The *k*-means clustering algorithm estimate the *k* mean values, which makes the within-cluster sum of squares (WCSS) minimum:

$$\arg\min_{S} \sum_{i=1}^{k} \sum_{x \in S_i} \|x - \mu_i\|^2 \tag{2}$$

Where μ_i is the mean value of i-th cluster and x is the speckle contrast values in an image frame.

The initial mean values could be randomly designated speckle contrast values within the image. Once the initial mean values are selected randomly, every speckle contrast values in the images are classified to the cluster of the least distance. The *k* clustered data sets computes new updated mean value and the new mean values classify the whole data again. The iterative operation ends when the updated mean values are within error tolerance.

Ultimate *k* clustered data sets play a role as nodal points in the form of the central point of each data set. The *k* centroids are computed for each speckle images in a time sequence. Because the camera has recorded the identical target objects, the centroids computed by different images are corresponded to each other if the number of mean values designated is equal. Consequently, the movement of clusters' centroids among time sequence image set is regarded as the displacement of the target object over time.

III. System identification using AR model

In the previous section, the sensing technique using the speckle pattern analysis is introduced and it successfully estimates the displacement of a target object. In structural engineering, the vibration measurement is mostly used for modal analysis applications. The modal analysis, which is the great analytical method to evaluate the dynamic properties, takes into account the overall stiffness of a structure. Since the structural damages imply the changes of stiffness in a structure, the modal analysis is practical SHM technique for damage assessment and detection process. For example, the frequency domain decomposition (FDD) is considered to be one of the most powerful and effective modal analysis techniques. FDD readily extracts modal parameters by decomposing the power spectral density matrix using the singular value decomposition.

In this section, system identification using AR model is introduced and modal parameters of the vibration signal obtained by the speckle pattern analysis are identified by two different ways: system identification using AR model and FDD. The AR model is a stochastic model, representing time series random signal process. Building AR model from the vibration signal obtained, AR coefficients (ARCs) are computed by burg's algorithm. Not only does the ARCs itself reflect the dynamic properties of the system, it is utilized to compute modal properties of the structure. The ARCs compose of the state matrix of the system and the modal parameters are computed by the eigenvalue decomposition of the state matrix.

This section explains the theoretical study on the output only operational modal analysis using system identification using AR model. To validate system identification using AR model, the simply simulated trigonometric functions signal is held up as an example. The AR model proves to extract the accurate ordinary frequency of the sine or cosine waves which the ordinary frequencies are pre-designated. The actual application of the vibration signal obtained by speckle pattern analysis will be covered in the next section for experimental method.

3.1 Autoregressive model and Burg's algorithm

In operational modal analysis, an observation of times series output vibration signal is needed. This study utilizes speckle patterns and a camera for the data observation and system identification using AR model is applied for extracting modal parameters, particularly natural frequency of a structure.

The AR model is the process of estimating the following stochastic value based on previous values. The output only AR model with model order p is defined as:

$$x(t) = \sum_{i=1}^{p} \phi_{ii} x(t-i) \tag{3}$$

Where, $\{\phi_{11}, \ldots, \phi_{pp}\}$ are the ARCs, $x(t\text{-}i)$ is the i-th time series signal and $x(t)$ is the AR estimation.

There are some different methods to estimate ARCs such as: Yule-Walker's algorithm and Burg's algorithm. According to the Introduction to Time Series and Forecasting by Brockwell, Burg's algorithm is considered to compute more probable coefficients than Yule-Walker's method. In this study, Burg's algorithm is utilized to estimate ARCs by minimizing forward and backward prediction errors. Once the time series observation data set $\{x_1, ..., x_n\}$ is obtained, the forward prediction errors $\{u_i(t)\}$ can be defined as:

$$u_0(t) = x_{n+1-t}, \tag{4}$$

$$u_i(t) = u_{i-1}(t-1) - \phi_{ii} v_{i-1}(t). \tag{5}$$

In the same manner, the backward prediction errors $\{v_i(t)\}$ are defined as:

$$v_0(t) = x_{n+1-t}, \tag{6}$$

$$v_i(t) = v_{i-1}(t) - \phi_{ii} u_{i-1}(t-1) \tag{7}$$

Burg's algorithm recursively estimates ARCs from ϕ_{11} to ϕ_{pp} by minimizing σ_{ii}^2. The generalized equations for computing ARCs $\{\phi_{11}, \ldots, \phi_{pp}\}$ are represented as:

$$d(1) = \sum_{t=2}^{n} (u_0^{\,2}(t-1) + v_0^{\,2}(t)) \tag{8}$$

$$\phi_{ii} = \frac{2}{d(i)} \sum_{t=i+1}^{n} v_{i-1}(t) u_{i-1}(t-1) \tag{9}$$

$$d(i+1) = (1-\phi_{ii}^{\,2}) d(i) - v_i^{\,2}(i+1) - u_i^{\,2}(n) \tag{10}$$

$$\sigma_i^2 = [(1-\phi_{ii}^2) d(i)] / [2(n-i)] \tag{11}$$

Where, ϕ_{ii} is i-th burg's estimate of ARC. The ARCs obtained by Equation (4) – (11) has stationary property if the time series output data is stationary. Therefore, the ARCs themselves are considered to reflect dynamic properties of a observed system and the change of the ARCs over time must state an any kind of structural changes or damages such as: degradation of material property, regional crack propagation along a concrete surface and structural defect in some structural elements.

3.2 Eigen-decomposition and modal identification

The ARCs computed by Burg's algorithm are used to build the state matrix of the system:

$$\Pi = \begin{pmatrix} \phi_{11} & \phi_{22} & \cdots & \phi_{p-1\,p-1} & \phi_{pp} \\ 1 & 0 & \cdots & 0 & 0 \\ 0 & 1 & \cdots & 0 & 0 \\ \vdots & \vdots & \ddots & \vdots & \vdots \\ 0 & 0 & \cdots & 1 & 0 \end{pmatrix}_{p\times p} \tag{12}$$

The eigendecomposition of the state matrix gives the modal parameters.

$$\Pi = L \begin{pmatrix} \pi_1 & 0 & \cdots & 0 \\ 0 & \pi_2 & \cdots & 0 \\ \vdots & \vdots & \ddots & \vdots \\ 0 & 0 & \cdots & \pi_p \end{pmatrix} L^{-1} \tag{13}$$

The diagonal elements of the eigenvalue matrix include natural frequency information. Natural frequency, mode shapes, and damping ratios of the system are respectively computed by Equation (14) – (16).

$$f_i = \frac{\sqrt{\mathrm{Re}^2(\lambda_i) + \mathrm{Im}^2(\lambda_i)}}{2\pi}; \text{where } \lambda = \frac{\ln(\pi_i)}{T_s} \tag{14}$$

$$\Psi = (\Psi_1 \quad \Psi_2 \quad \cdots \quad \Psi_p) = (1 \quad 0 \quad \cdots \quad 0)L \tag{15}$$

$$\zeta_i = -\frac{\mathrm{Re}(\lambda_i)}{2\pi f_i} \tag{16}$$

The multiple autoregressive models built by multiple vibration signals constitute larger size state matrix. With m signals, the ARCs obtained from m autoregressive model each compose *mp*×*mp* size of state matrix:

$$\Pi = \begin{pmatrix} \Phi^{(1)}_{m\times m} & \Phi^{(2)}_{m\times m} & \cdots & \Phi^{(\mathrm{p}-1)}_{m\times m} & \Phi^{(\mathrm{p})}_{m\times m} \\ I_{m\times m} & 0 & \cdots & 0 & 0 \\ 0 & I_{m\times m} & \cdots & 0 & 0 \\ \vdots & \vdots & \ddots & \vdots & \vdots \\ 0 & 0 & \cdots & I_{m\times m} & 0 \end{pmatrix}_{(m\times p)\times(m\times p)} \tag{17}$$

$$\text{where, } \Phi^{(i)} = \begin{pmatrix} \phi_1^{(ii)} & 0 & \cdots & 0 \\ 0 & \phi_2^{(ii)} & \cdots & 0 \\ \vdots & \vdots & \ddots & \vdots \\ 0 & 0 & \cdots & \phi_m^{(ii)} \end{pmatrix}_{m\times m}$$

3.3 Stationary property of ARCs

The ARCs includes dynamic properties of a measured system and the eigendecomposition of the state matrix composed of ARCs gives modal properties. If a structure are not damaged and the dynamic property of the structure remains constant, the time series output data measured on a structure has stationary property over time. However, if the structure is damaged, its stiffness and damping ratios are changed over time. The change of stiffness and damping ratios affects the dynamic response of the structure and it consequently changes ARCs. In theory, the ARCs computed by stationary data set will be consistent if other conditions like model order, data length, and experimental environment are constant. Since the real measurements are inevitably affected by a lot of variables, the ARCs obtained from stationary vibration responses remain constant over time within a mean value and standard deviation. Therefore, a change of the ARCs over time states that damages has been occurred within the structure, such as: regional defects, degradation of the structural materials, or damages in structural elements.

3.4 Example

In this section, system identification using AR model is applied to simple trigonometric functions simulated in Matlab. Since the ordinary frequency of simulated trigonometric fuction is adjustable by user, system identification using AR model is expected to extract the probable result. The two simulated trigonometric functions are given as examples to prove the methodology; one is a single cosine function, which has one ordinary frequency and the other is a sum of four cosine functions, which has four different ordinary frequencies. The detailed information about the functions is shown in Table 1. The ordinary frequencies of two samples are pre-designated and the magnitudes and phases in the cosine functions are randomly selected in uniformly distributed numbers between 0 and 1. The sampling frequency of both samples is equal to 30 Hz and the ARCs of simulated data are calculated by burg's algorithm with model order from 1 to 500.

Table 1 The simulated trigonometric function

	A single cosine function	**A sum of trigonometric functions**
Function	$y = \cos(6.4\pi \cdot t)$	$y = rand \cdot \cos\left(5.04\pi \cdot (t - rand)\right) + rand \cdot \cos\left(9.02\pi \cdot (t - rand)\right) + rand \cdot \cos\left(15.98\pi \cdot (t - rand)\right) + rand \cdot \cos\left(22.94\pi \cdot (t - rand)\right)$
Sampling frequency	30Hz	30 Hz
Ordinary frequencies	3.2Hz	2.52 Hz, 4.51 Hz, 7.99 Hz and 11.47 Hz
Model order	From 1 to 500	From 1 to 500

The simulated signals based on Table 1 are shown in Figure 3 and Figure 4. Each signal builds AR model and the burg's algorithm computes burg's estimation of ARCs. The eigendecomposition of the state matrix composed of ARCs gives ordinary frequency information. The generated signals are expected to compute the pre-designated ordinary frequency through the methodology.

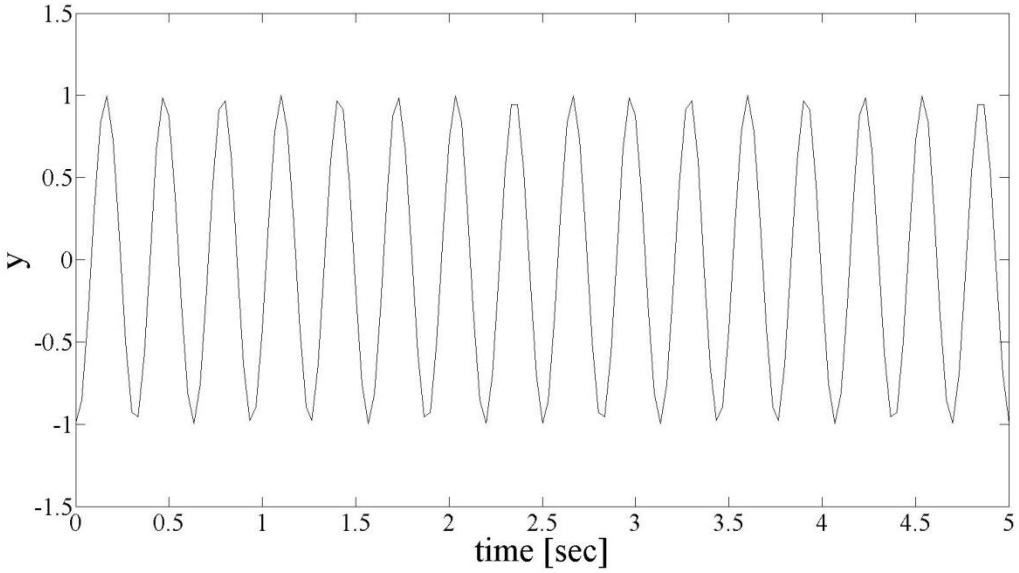

Figure 3 The signal of a single cosine function

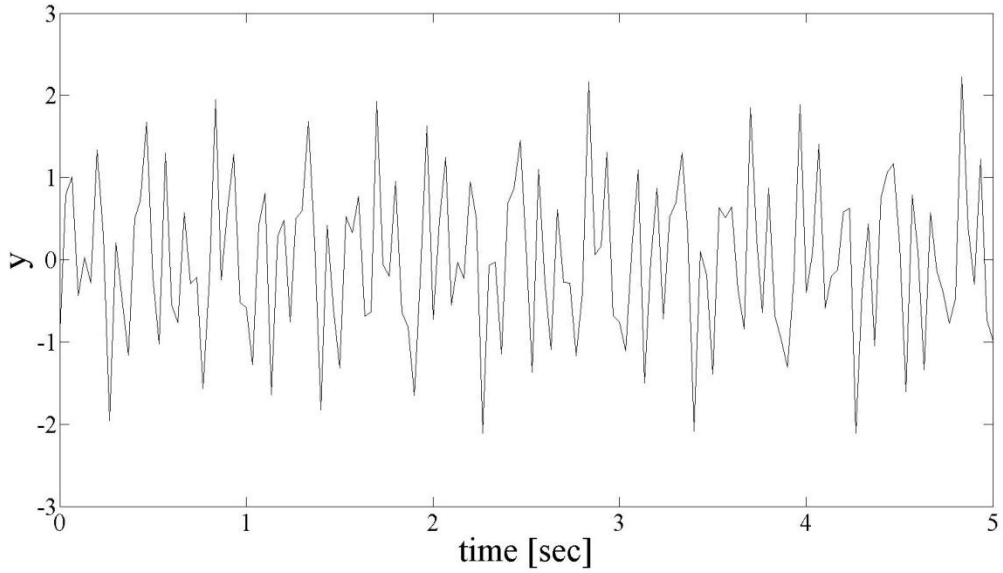

Figure 4 The signal of the sum of cosine functions

3.4.1 Results

Figure 5 and Figure 6 are the graph of the ordinary frequency computed from eigenvalues of the state matrix. The ordinary frequency information is plotted along the model order. The plotted eigenvalues have a convergent trend where the section of ordinary frequency exists. The system identification using AR model extracted the ordinary frequencies of both cosine functions.

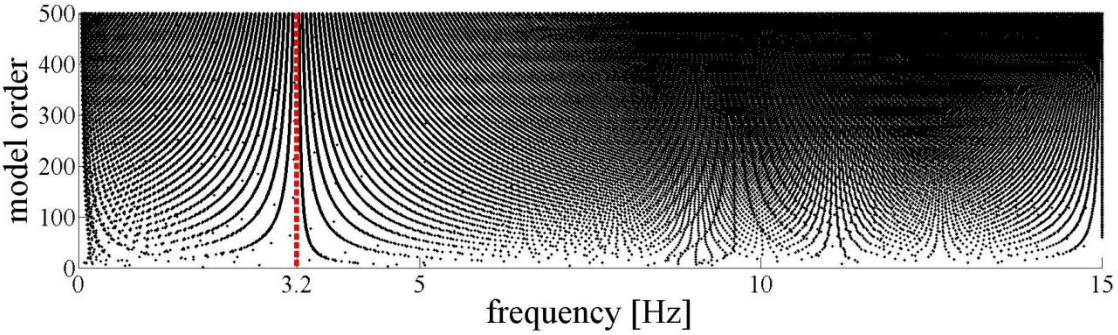

Figure 5 Ordinary frequency extracted from the single cosine function

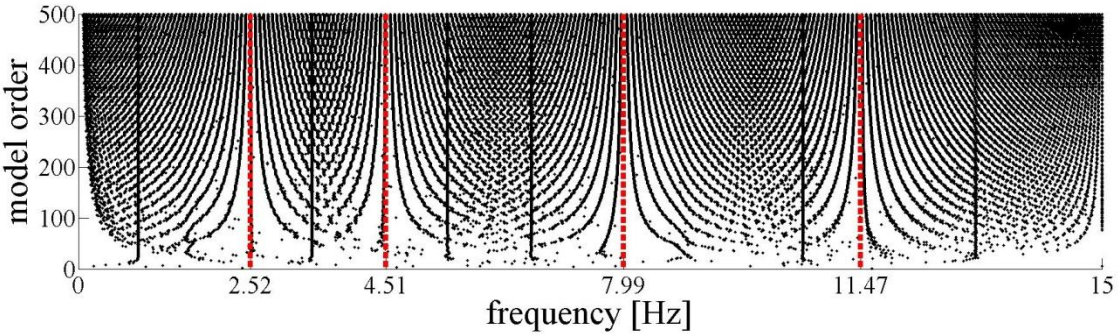

Figure 6 Ordinary frequency extracted from the sum of 4 cosine functions

IV. Experiments

Two experiments were conducted to validate the speckle pattern recognition analysis. The displacement signals obtained from the speckle pattern recognition analysis are decomposed to the frequency domain through both FDD and system identification using AR model. The first experiment was to obtain speckle patterns from the steel plate on a shaker. A camera records the speckle pattern created from the steel plate and the steel plate is vibrating with the pre-assigned shaking frequency of the shaker. This experiment proves that the speckle pattern obtained by the photographic camera. In the second experiment, the target object was the small steel beam model. The second experiment proves that the speckle pattern recognition analysis appropriately detects the ambient vibrations of structures.

The frame rate of two experiments was 30 frames per seconds; the fps is equivalent to sampling frequency in vision-based speckle pattern recognition algorithm, so the Nyquist frequency of both experiments is 15 Hz. Since the targeting frequencies for two experiments are within 15Hz, 30 fps is enough for each experiment. The speckle contrast of the pixel is the standard deviation of speckle intensities divided by the means of speckle intensities within a speckle window. The size of speckle window used in two experiments is 7×7. Therefore, the speckle contrast of a certain pixel represents the standard deviation divided by the mean of speckle intensities of 3 pixels before and after the pixel of interest. Figure 7 below demonstrates the speckle contrast. The three external pixel layers are exempt from the speckle contrast calculation because the pixels don’t have enough speckle window size.

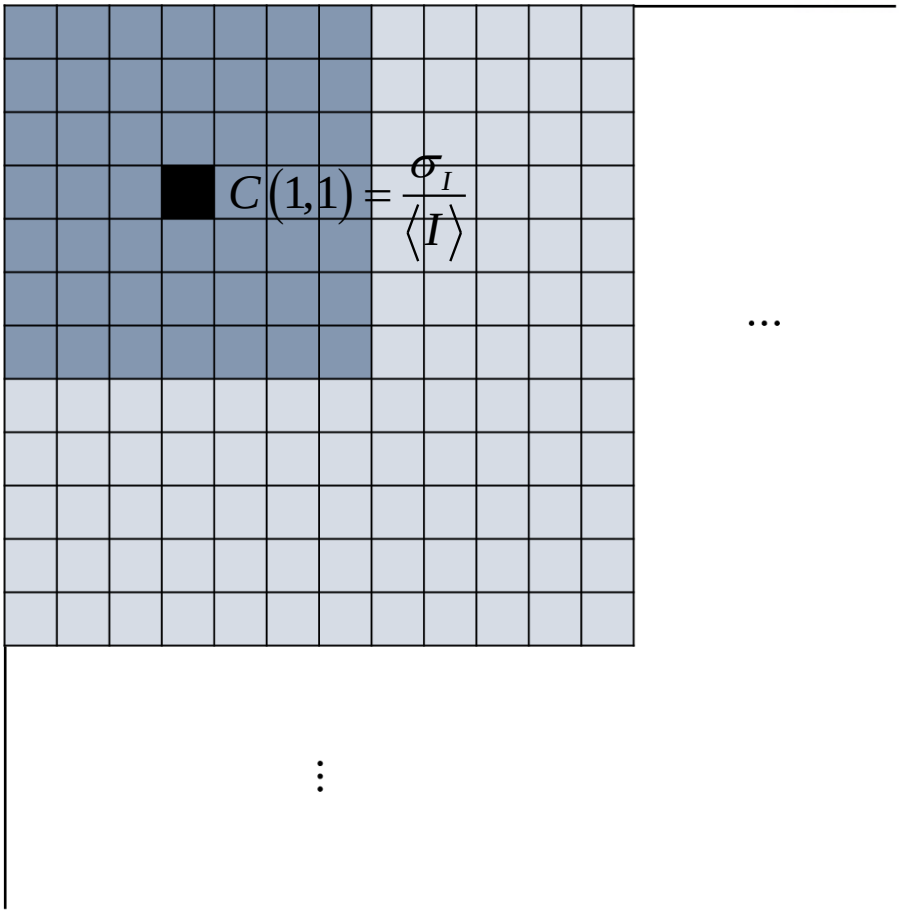

Figure 7 Speckle contrast imaging

4.1 Shaker and steel plate

The first experiment was conducted with a shaker and a steel plate. The purpose of this experiment was to check if the speckle pattern recognition algorithm reflects the pre-designated frequency of the shaker. While the shaker vibrated the steel plate with assigned frequency, the laser pointer was spread over the steel plate and a camera was recording the speckle pattern created from the steel plate. Figure 8 shows the experimental setup. The steel plate moves perpendicular to the camera angle and the camera captures the speckle patterns with 30 fps frame rate. The total data length of each experimental trial was 256. The experiment was conducted 4 times with different vibrating frequency: 2 Hz, 3 Hz, 4 Hz, and 5 Hz. The linear variable differential transformer (LVDT) measures the displacement of the steel plate to prove the vibrating frequencies.

The LASCA highlights the movement of the steel plate by quantifying the blurring in the image frame and *k*-means clustering of the speckle contrast values in each image frame gives virtual nodal points. The movement of the virtual nodal points in a pixel frame is considered to be the displacement of the steel plate and frequency decomposition techniques gives frequency of the target, which will corresponds to the pre-designated vibrating frequency. In this experiment, the number of clusters is designated as twenty. One cluster is selected for each experimental trial and the FFT of the signal is compared to the FFT result of the LVDT signal of corresponding excitation. The results of the experiment are shown as a fast Fourier transformation (FFT) graph of displacement signal from both LVDT and the speckle patterns: Figure 9 - Figure 16. The FFT results of clusters' centroid of speckle patterns have a peak point at the corresponding frequency of exciting frequency.

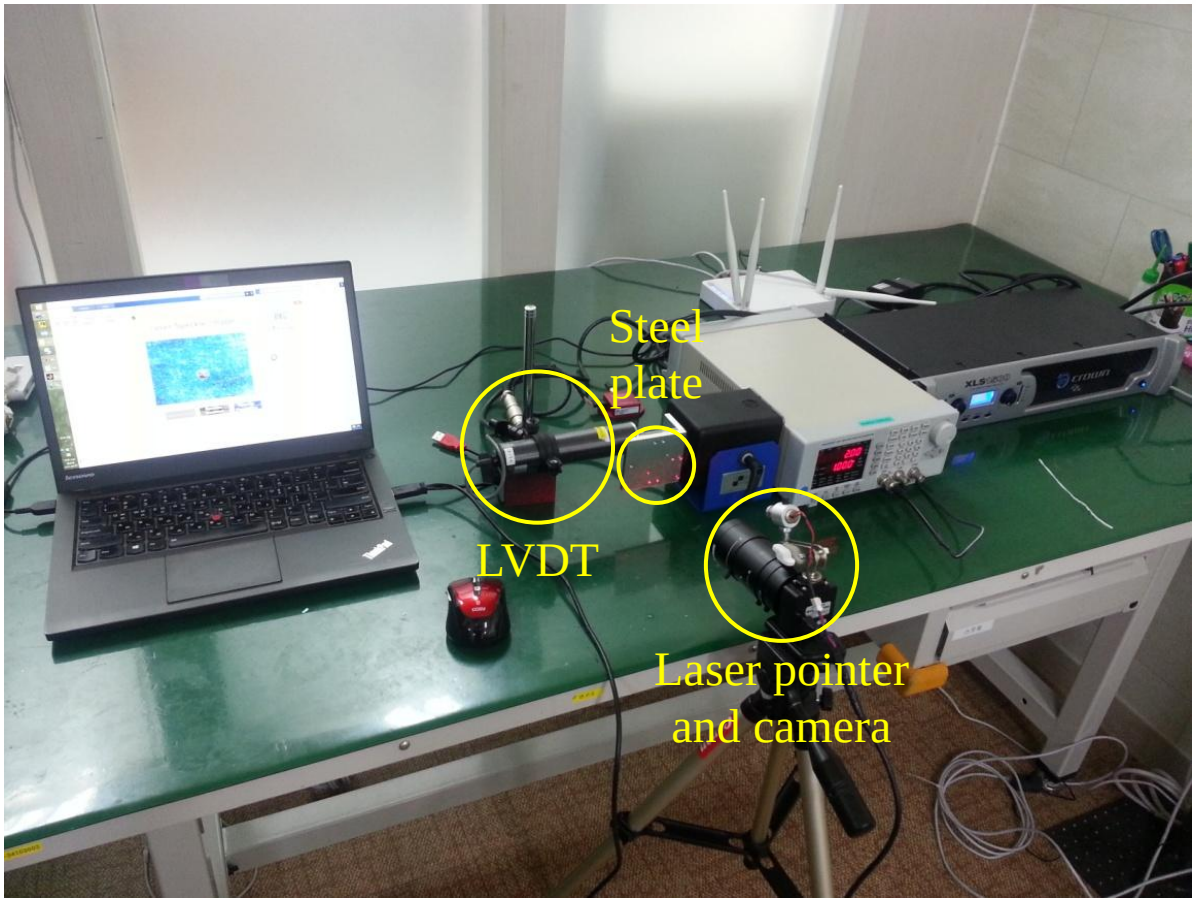

Figure 8 Shaker and steel plate

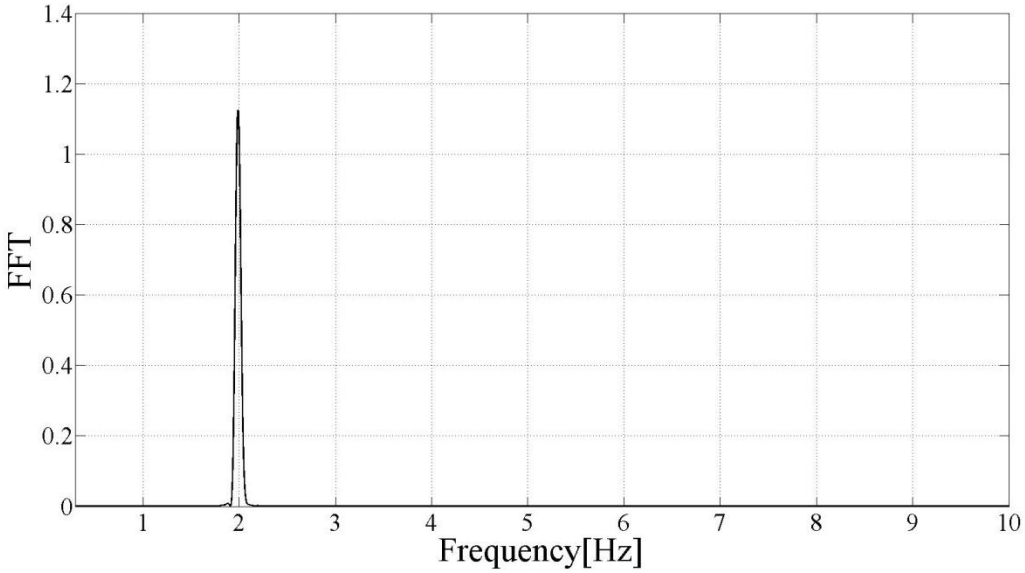

Figure 9 Fast Fourier transform of a displacement obtained by LVDT; shaking frequency: 2 Hz

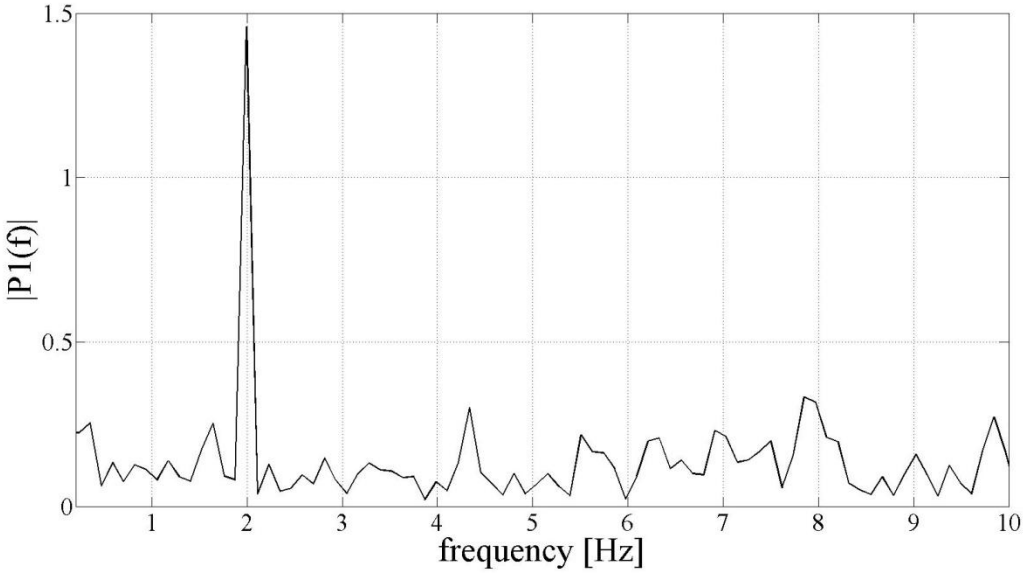

Figure 10 Fast Fourier transform of a steel plate's speckle centroid; shaking frequency: 2 Hz

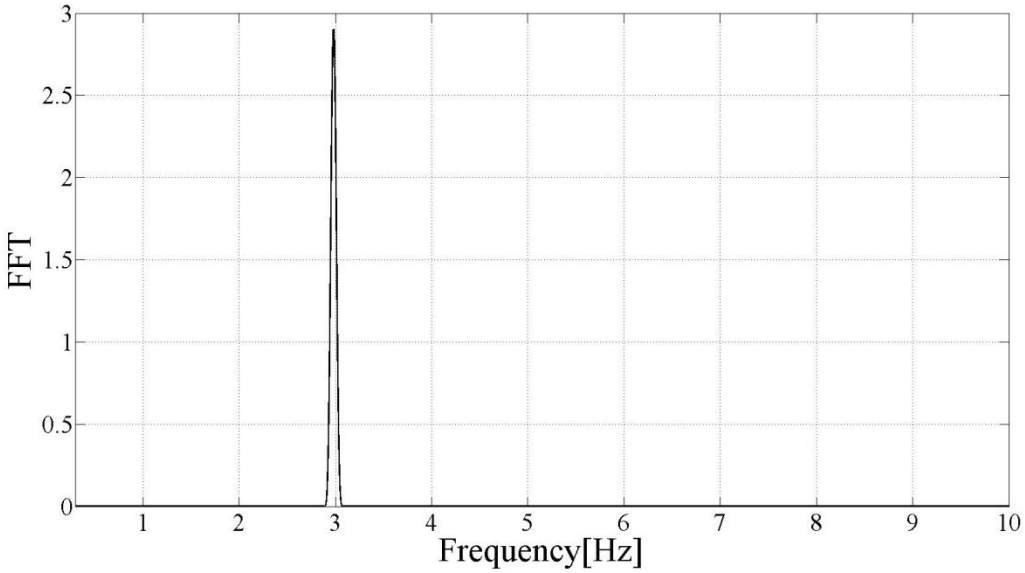

Figure 11 Fast Fourier transform of a displacement obtained by LVDT; shaking frequency: 3 Hz

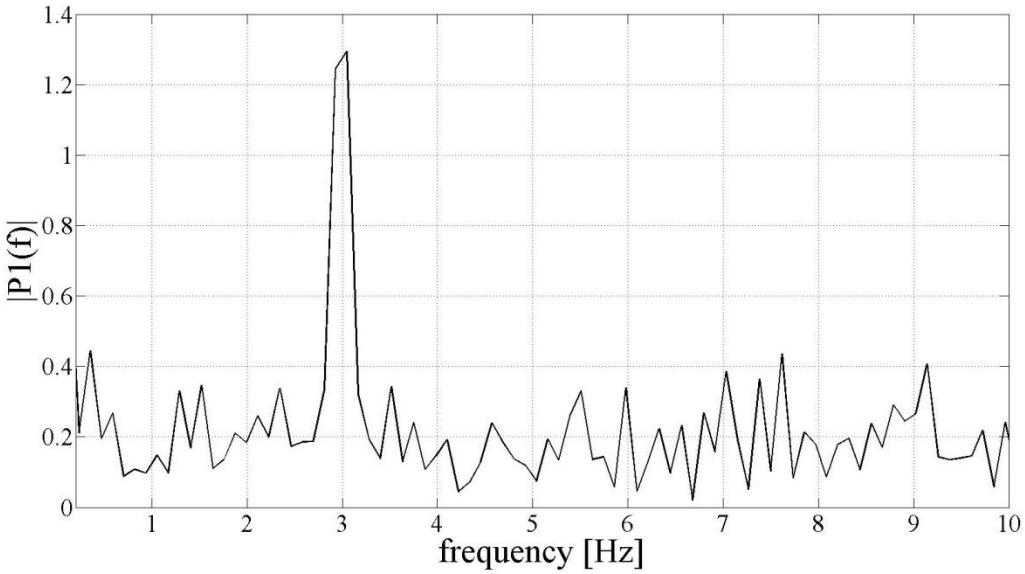

Figure 12 Fast Fourier transform of a steel plate's speckle centroid; shaking frequency: 3 Hz

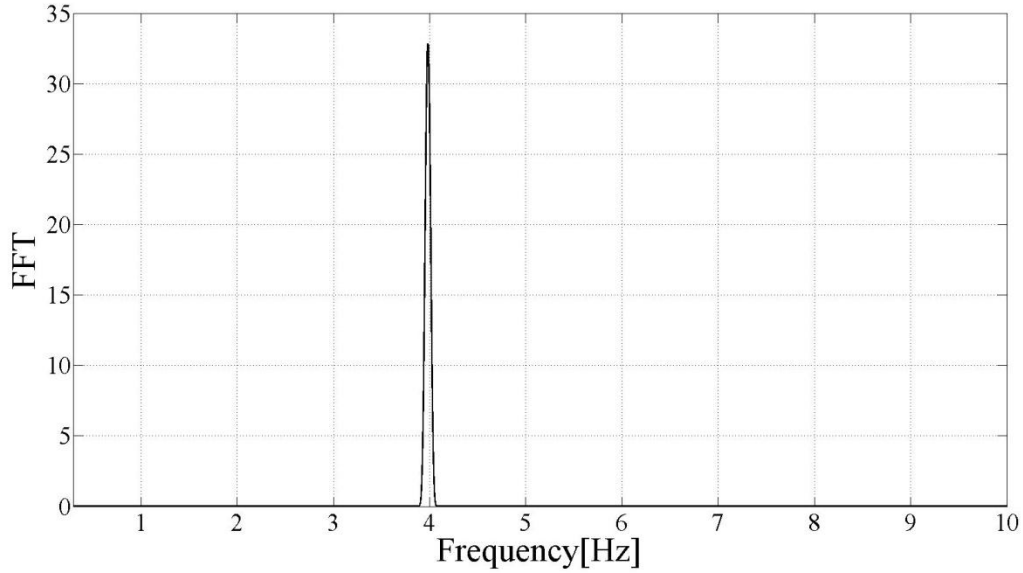

Figure 13 Fast Fourier transform of a displacement obtained by LVDT; shaking frequency: 4 Hz

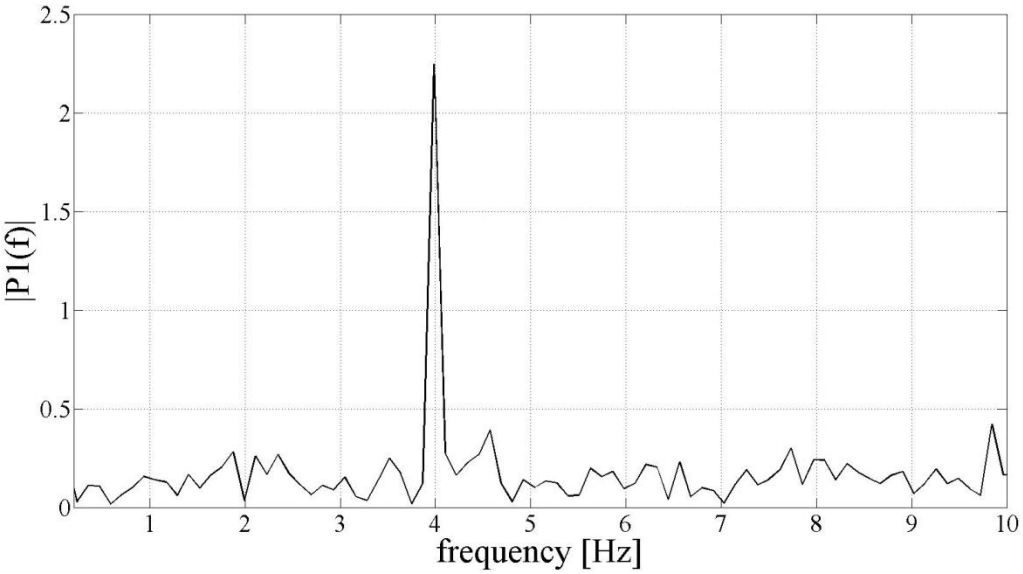

Figure 14 Fast Fourier transform of a steel plate's speckle centroid; vibrating frequency: 4 Hz

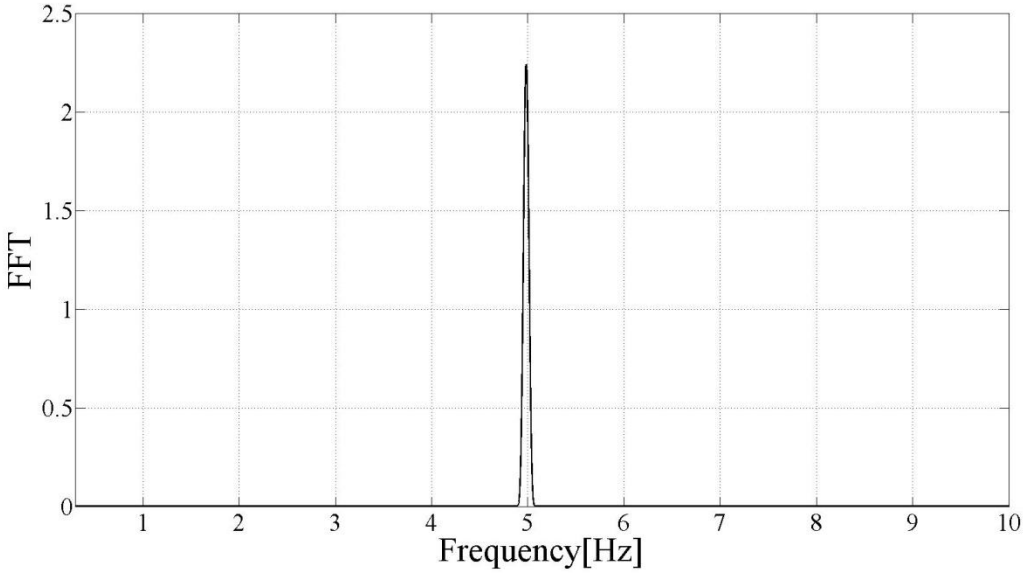

Figure 15 Fast Fourier transform of a displacement obtained by LVDT; shaking frequency: 5 Hz

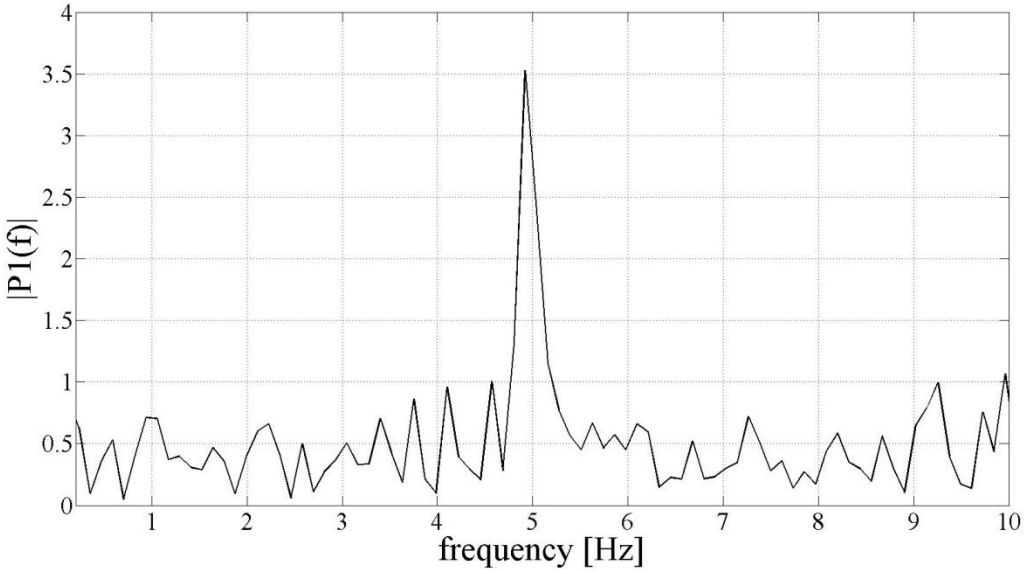

Figure 16 Fast Fourier transform of a steel plate's speckle centroid; vibrating frequency: 5 Hz

4.2 Steel beam model

The second experiment was done with a short steel beam model shown in Figure 17. The steel beam has 0.01 m × 0.1m of cross section property and the total length of the beam is 2 m. The experimental setup including the laser pointer and the web camera shown in Figure 18 aimed for the beam's side of the center. A short-duration impulse was applied to the beam and the camera recorded the changes of speckle pattern created from the center of the beam due to the ambient vibration of the beam. The frame rate of the web camera was 30 fps. Because the targeting frequency of the experiment was within 15 Hz, 30 fps is enough sampling frequency for this experiment. The experiments were conducted 2 times; the first was done in bright circumstance and the other was done in dark circumstance. The experiment proved the speckle pattern recognition technique was also available in night time. The total data length of each experimental trial is 1800 which means the number of speckle images from the steel beam is 1800 and the images are taken in 60 seconds.

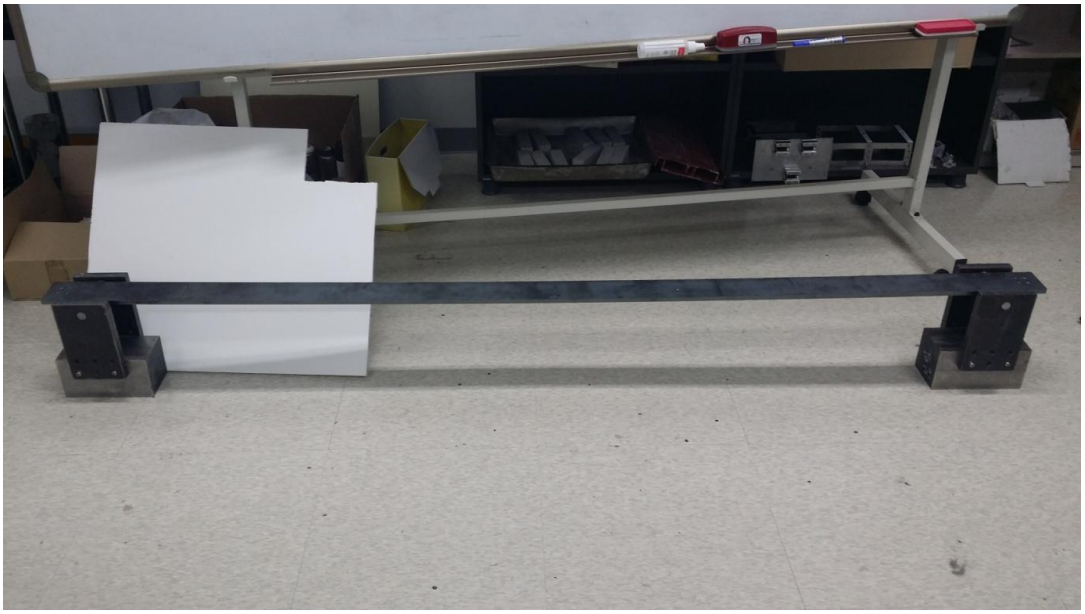

Figure 17 Steel beam model

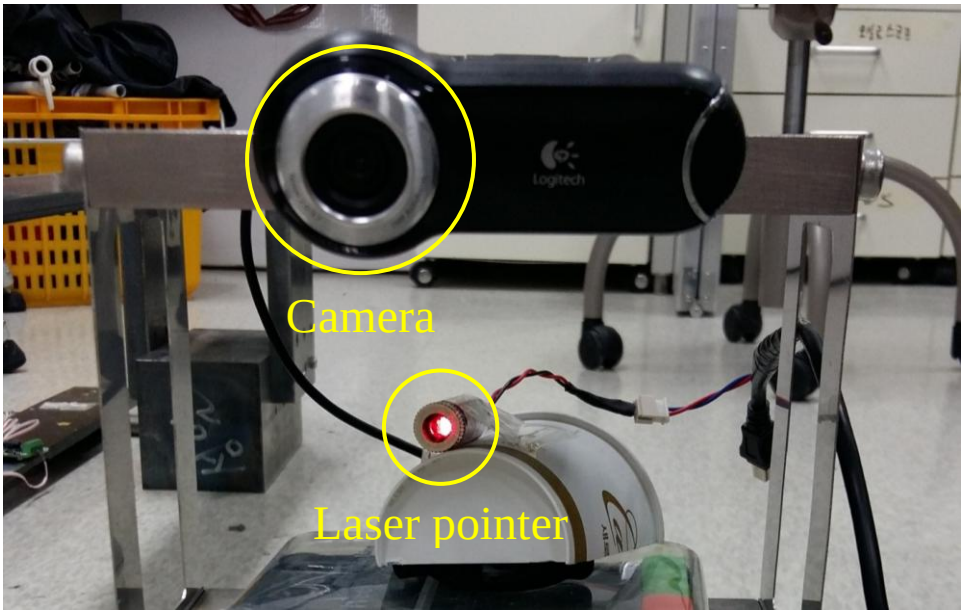

Figure 18 Camera and laser pointer

The raw speckle images are shown in Figure 19 and Figure 20Figure 20. The figures are the raw speckle pattern created from the center of the beam and the camera is targeting the center of the beam. The rectangular cylinder on the Figure 19 and Figure 20 is the speckle image of the beam model. Figure 19 is a speckle image in static moment and Figure 20 is a speckle image in dynamic moment. The blurring effect in Figure 20 states that there is a movement of the beam at the moment. The speckle contrast is used to quantify the movement in a stationary image using equation (1).

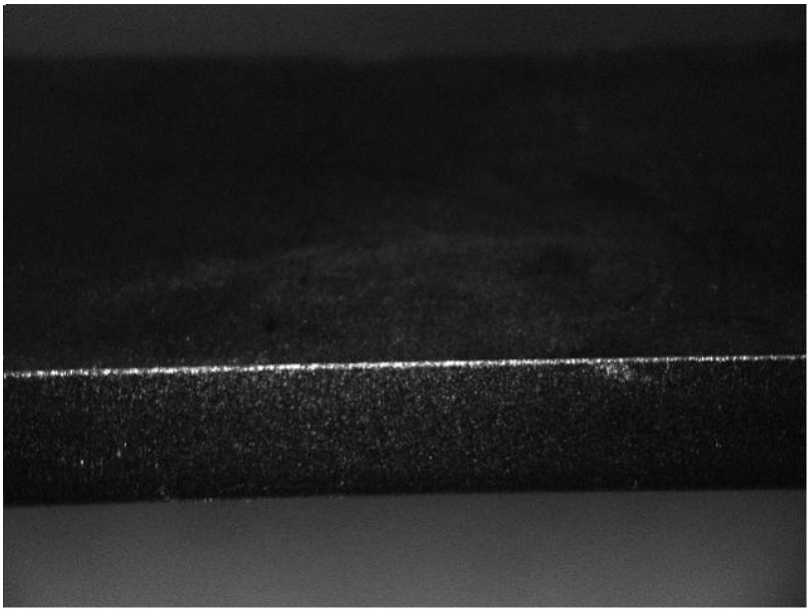

Figure 19 Raw speckle image in static moment

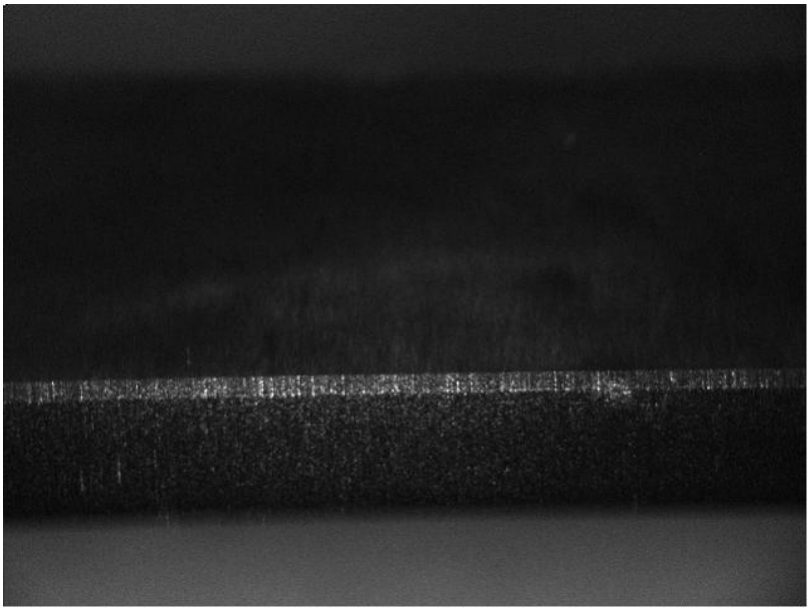

Figure 20 Raw speckle image in dynamic moment

Figure 21 and Figure 22 are the speckle contrast image in static moment and the speckle contrast image in dynamic moment respectively. Since speckle contrast values are less when blurring happens, the average speckle contrast value of speckle contrast image in dynamic moment is less than the average speckle contrast value of speckle contrast image in static moment.

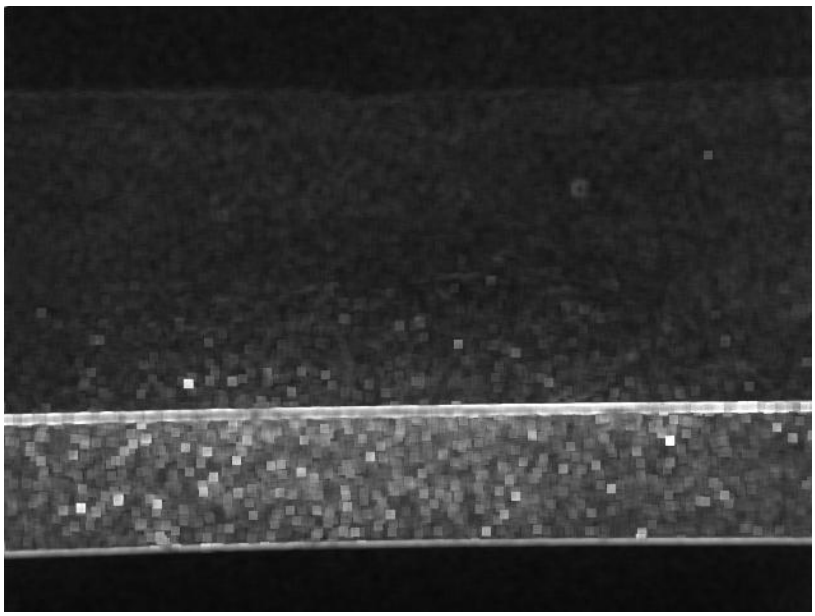

Figure 21 Speckle contrast image in static moment

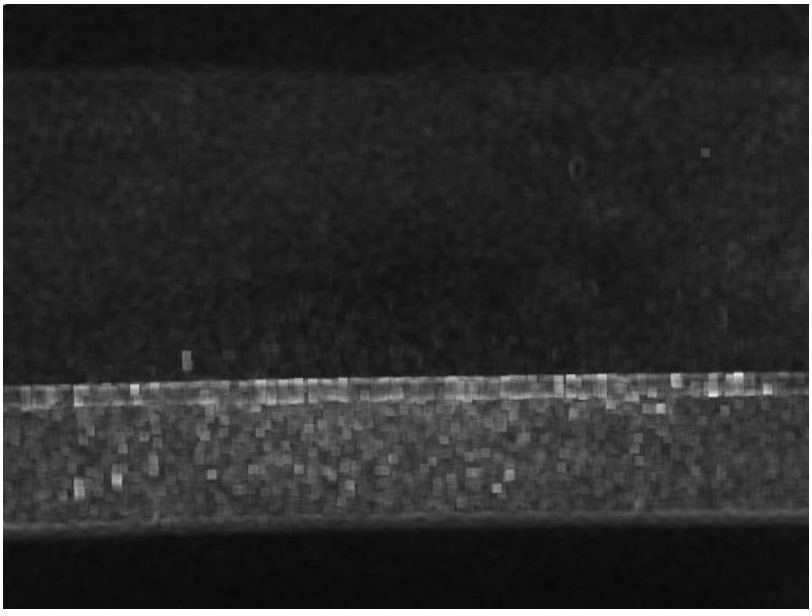

Figure 22 Speckle contrast image in dynamic moment

The speckle contrast imaging technique successfully digitalize the movement in image frames. The next step is to classify the speckle contrast values in each image by k-means clustering algorithm. In this experiment, the speckle contrast images were classifies with 5 clusters. It is probable to set larger number of clusters but k-mean clustering algorithm for large number of images is computationally expensive process. Since the scope of this experiment is to prove if the speckle pattern recognition technique properly refect an ambient vibration of the steel beam, 5 clusters are enough. Figure 23, Figure 24, Figure 25, and Figure 26 are the horizontal or vertical movement of cluster's centroid in bright or dark condition. The displacement also can be computed by considering the ratio between pixel distance and the acutual geometry. Instead, this study requires only the vibration signal in time domain for decomposing it into frequency domain. Therefore the location signals themselves are enough.

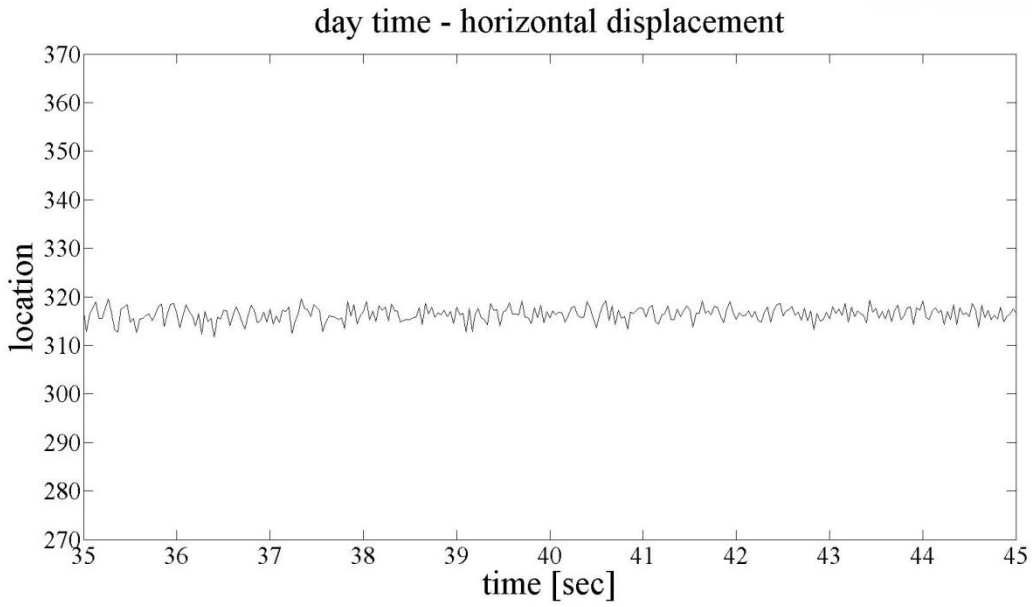

Figure 23 Location changes of cluster's centroid along horizontal direction in bright condition

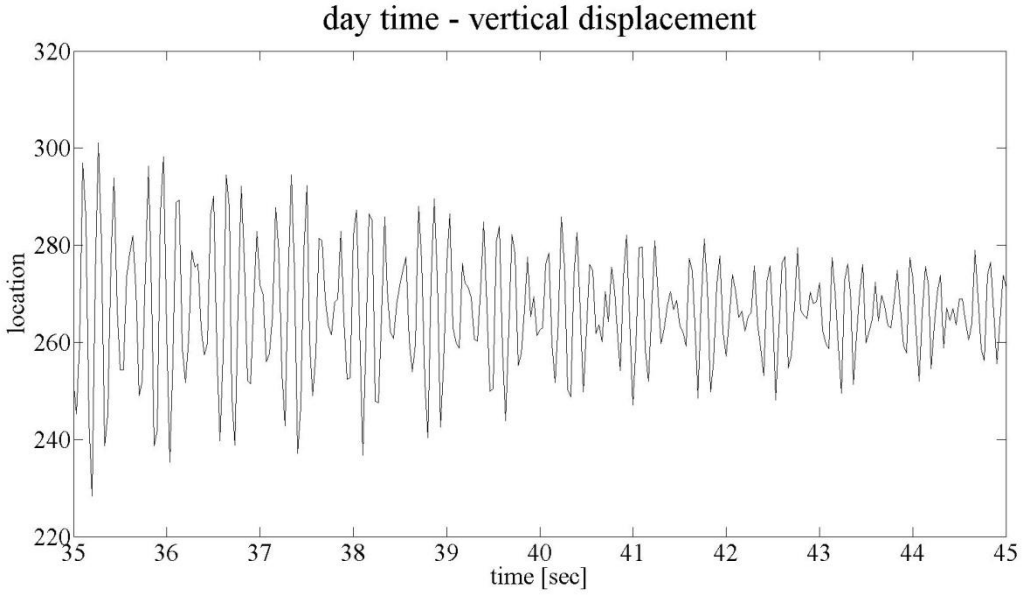

Figure 24 Location changes of cluster's centroid along vertical direction in bright condition

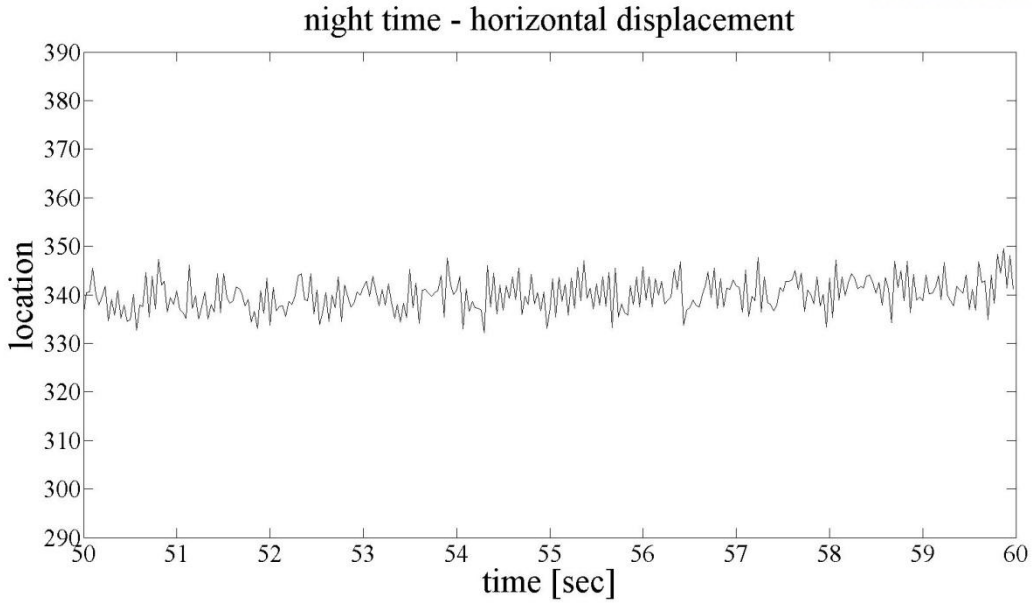

Figure 25 Location changes of cluster's centroid along horizontal direction in dark condition

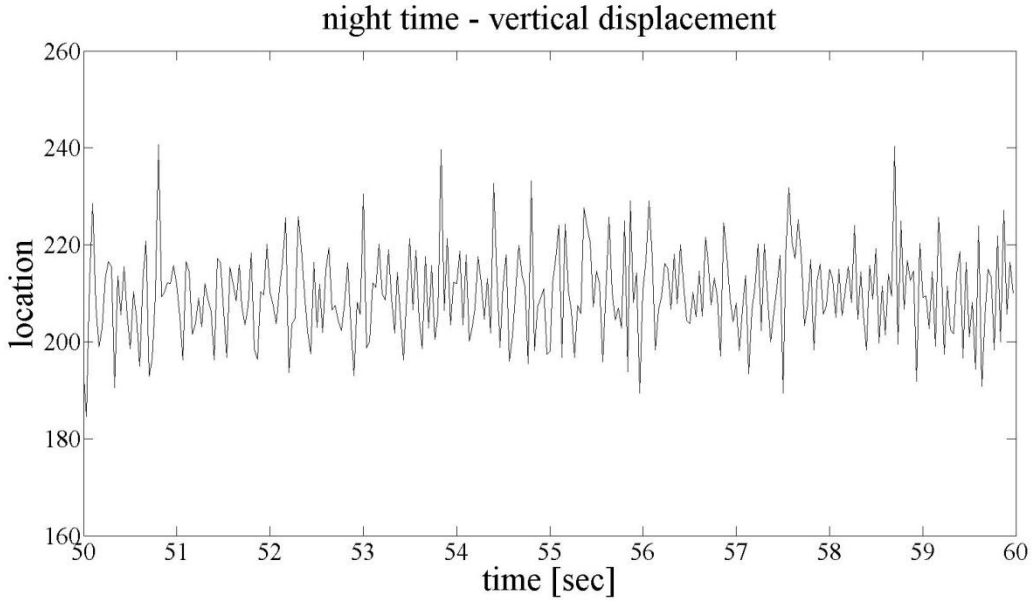

Figure 26 Location changes of cluster's centroid along vertical direction in bright condition

To compute the dynamic property of the target, FDD algorithm and system identification using AR model are applied to the vibration signal obtained by speckle pattern recognition algorithm. Figure 27, Figure 28, Figure 29, and Figure 30 are respectively the FDD result of Figure 23, Figure 24, Figure 25, and Figure 26. In Figure 28, the result clearly shows that there is a clear significant peak at 5.859 Hz in the frequency domain. The normal mode of the steel beam has 5.859 Hz of natural frequency.

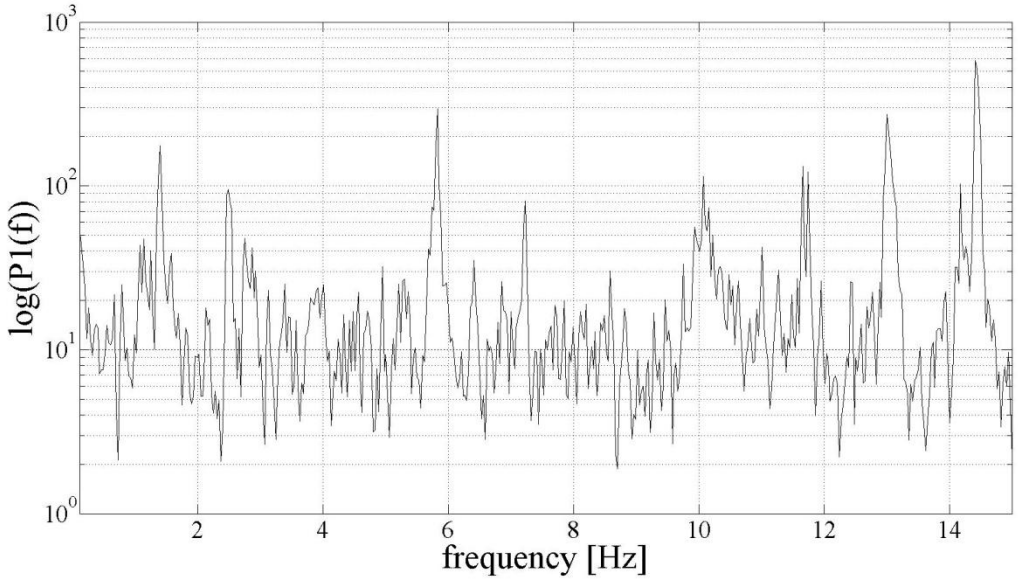

Figure 27 FDD of the centroids of speckle clusters along horizontal direction in bright condition

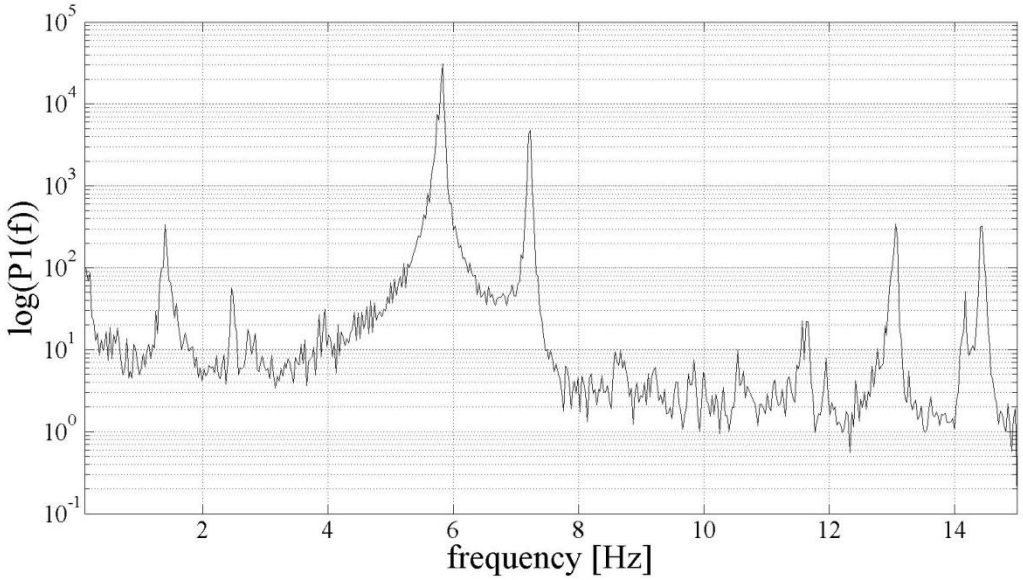

Figure 28 FDD of the centroids of speckle clusters along vertical direction in bright condition

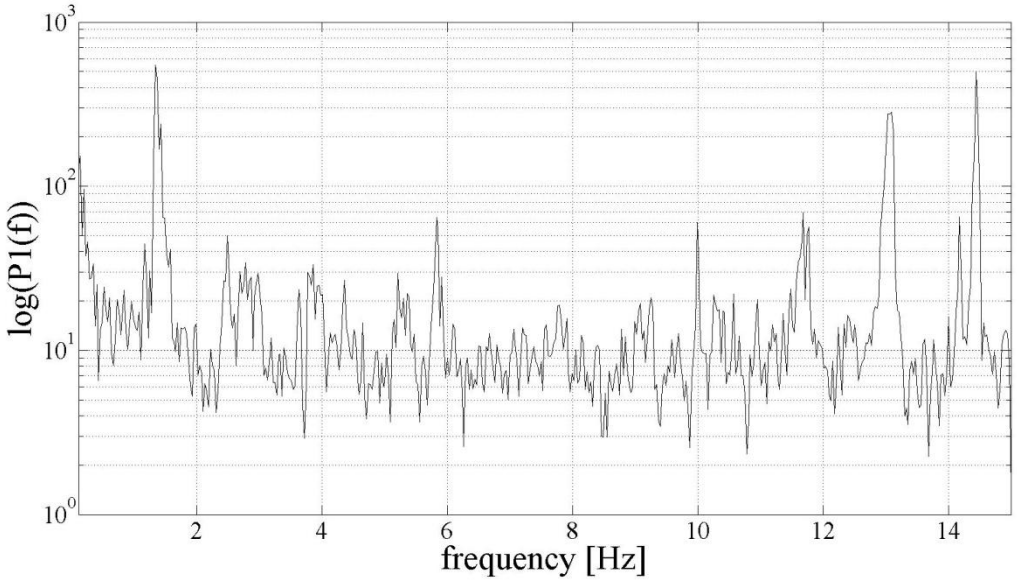

Figure 29 FDD of the centroids of speckle clusters along horizontal direction in dark condition

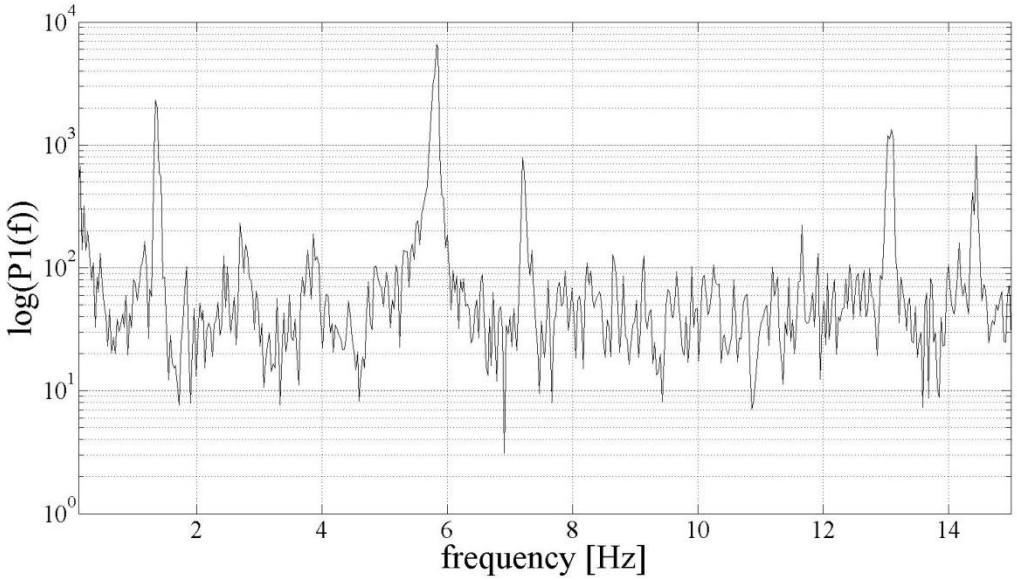

Figure 30 FDD of the centroids of speckle clusters along horizontal direction in dark condition

The other modal identification method used in this study is system identification using AR model. The vibration data obtained by k-means clustering algorithm are put into the burg's algorithm from equation (4) to equation (11). The AR coefficients computed by burg's algorithm compose of the state matrix as shown in equation (17). The natural frequency is obtained by the eigendecomposition of the state matrix: equation (13) and equation (14). In this experiment, one cluster's centroid was selected because system identification using AR model with 5 signals requires intensive computational process and it takes a long time to executive a whole algorithm with normal computer. Figure 31 and Figure 32 are the frequency domain result of system identification using AR model. There is a clear convergence on 5.823 Hz.

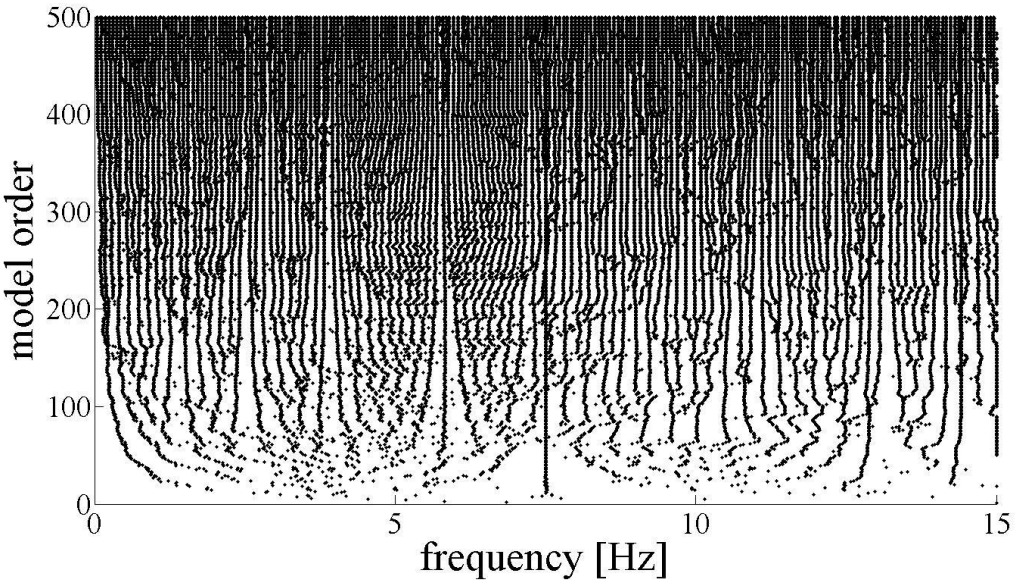

Figure 31 Frequency domain result of the system identification using AR model

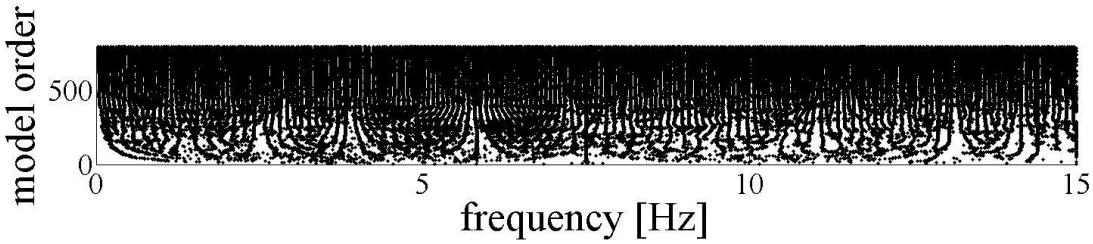

Figure 32 Squeezed graph of Figure 31

V. Conclusion

This study proved that the laser speckle pattern analysis can be applied to the structural health monitoring (SHM) in civil engineering and it can detect the modal properties of the target structure. Visual based SHM methods are not new in civil engineering but either they require a target panel or have an inferior accuracy. The speckle pattern is sensitive to any vibration of the target structure and the *k*-means clustering algorithm can classify the speckle flow image from the several frames taken per second. The *k* numbers of clusters' centroids play the role of virtual nodes. From the signals created in time domain by these virtual nodes any system identification algorithm can extract meaningful results in frequency domain. The experimental results demonstrate that with an inexpensive laser pointer and an inexpensive camera it is possible to monitor structures by analyzing a laser speckle pattern.

If these experiments are performed with more expensive equipment, more sensitive and minute observations are expected. For example, the structural monitoring of a steel bridge at a few thousand feet away from the bridge is feasible with the use of a high quality camera and a high energy laser pointer. In addition, SHM of physically inaccessible structures is possible, such as: the monitoring of the center span of a bridge crossing a river from one of the embankments, or the monitoring of a steel pipe running through a protected or inaccessible area. The range of applications of this method is not limited to civil engineering.

In the future, more sensitive speckle pattern experiments in harsher experimental condition will be performed to validate this technology broadly. Multi camera systems will be developed to allow the extraction of the mode shapes.

References

An, Y. K., Park, B., & Sohn, H. (2013). Complete noncontact laser ultrasonic imaging for automated crack visualization in a plate. *Smart Materials and Structures, 22*(2). doi:Artn 02502210.1088/0964-1726/22/2/025022

Briers, J. D., & Webster, S. (1996). Laser speckle contrast analysis (LASCA): a nonscanning, full-field technique for monitoring capillary blood flow. *Journal of biomedical optics, 1*(2), 174-179.

Brincker, R., Zhang, L., & Andersen, P. (2000). *Modal identification from ambient responses using frequency domain decomposition*. Paper presented at the Proc. of the 18*'International Modal Analysis Conference (IMAC), San Antonio, Texas.

Chang, P. C., Flatau, A., & Liu, S. (2003). Review paper: health monitoring of civil infrastructure. *Structural health monitoring, 2*(3), 257-267.

Dunn, A. K., Bolay, H., Moskowitz, M. A., & Boas, D. A. (2001). Dynamic imaging of cerebral blood flow using laser speckle. *Journal of Cerebral Blood Flow & Metabolism, 21*(3), 195-201.

Goodman, J. W. (1976). Some Fundamental Properties of Speckle. *Journal of the Optical Society of America, 66*(11), 1145-1150. doi:Doi 10.1364/Josa.66.001145

Hartigan, J. A., & Wong, M. A. (1979). Algorithm AS 136: A k-means clustering algorithm. *Journal of the Royal Statistical Society. Series C (Applied Statistics), 28*(1), 100-108.

Köpf, U. (1972). Application of speckling for measuring the deflection of laser light by phase objects. *Optics Communications, 5*(5), 347-350.

Lee, J. J., & Shinozuka, M. (2006). A vision-based system for remote sensing of bridge displacement. *Ndt & E International, 39*(5), 425-431. doi:10.1016/j.ndteint.2005.12.003

Leendertz, J., & Butters, J. (1973). An image-shearing speckle-pattern interferometer for measuring bending moments. *Journal of Physics E: Scientific Instruments, 6*(11), 1107.

Lynch, J. P., & Loh, K. J. (2006). A summary review of wireless sensors and sensor networks for structural health monitoring. *Shock and Vibration Digest, 38*(2), 91-130.

Park, K., Kim, S., & Torbol, M. (2016). Operational modal analysis of reinforced concrete bridges using autoregressive model. *Smart Structures and Systems, 17*(6), 1017-1030. doi:10.12989/sss.2016.17.6.1017

Rabal, H. J., & Braga Jr, R. A. (2008). *Dynamic laser speckle and applications*: CRC Press.

Sohn, H., Farrar, C. R., Hemez, F. M., Shunk, D. D., Stinemates, D. W., Nadler, B. R., & Czarnecki, J. J. (2003). A review of structural health monitoring literature: 1996–2001. *Los Alamos National Laboratory, USA*.

Vest, C. M. (1979). Holographic interferometry. *New York, John Wiley and Sons, Inc., 1979. 476 p., 1*.

Yang, L. X., & Ettemeyer, A. (2003). Strain measurement by three-dimensional electronic speckle pattern interferometry: potentials, limitations, and applications. *Optical Engineering, 42*(5), 1257-1266. doi:10.1117/1.1566781